Biogeosciences Discuss., 12, 9613–9650, 2015
www.biogeosciences-discuss.net/12/9613/2015/
doi:10.5194/bgd-12-9613-2015

Biogeosciences
Discussions
Open Access

Precipitation legacy effects on dryland ecosystem carbon fluxes: direction, magnitude and biogeochemical carryovers

W. Shen[1], G. D. Jenerette[2], D. Hui[3], and R. L. Scott[4]

[1]Key Laboratory of Vegetation Restoration and Management, South China Botanical Garden, the Chinese Academy of Sciences, Guangzhou, 510650, China
[2]Department of Botany and Plant Sciences, Center for Conservation Biology, University of California Riverside, Riverside, CA92521, USA
[3]Department of Biological Sciences, Tennessee State University, Nashville, TN 37209, USA
[4]USDA-Agricultural Research Service, Southwest Watershed Research Center, Tucson, AZ 85719, USA

Received: 05 June 2015 – Accepted: 08 June 2015 – Published: 01 July 2015

Correspondence to: W. Shen (shenweij@scbg.ac.cn)

Published by Copernicus Publications on behalf of the European Geosciences Union.

Abstract

The precipitation legacy effect, defined as the impact of historical precipitation (PPT) on extant ecosystem dynamics, has been recognized as an important driver in shaping the temporal variability of dryland aboveground primary production (ANPP) and soil respiration. How the PPT legacy influences whole ecosystem-level carbon (C) fluxes has rarely been quantitatively assessed, particularly at longer temporal scales. We parameterized a process-based ecosystem model to a semiarid savanna ecosystem in southwestern US, calibrated and evaluated the model performance based on 7 years of eddy covariance measurements, and conducted two sets of simulation experiments to assess interdecadal and interannual scale PPT legacy effects over a 30 year simulation period. The results showed that decreasing the previous period/year PPT (dry legacy) always imposed positive impacts on net ecosystem production (NEP) whereas increasing the previous period/year PPT (wet legacy) had negative impacts on NEP. The simulated dry legacy impacts were mostly positive on gross ecosystem production (GEP) and negative on ecosystem respiration (R_e) but the wet legacy impacts were mostly negative on GEP and positive on R_e. Although the direction and magnitude of GEP and R_e responses to the simulated dry and wet legacies were influenced by both the previous and current PPT conditions, the NEP responses were predominantly determined by the previous PPT characteristics including rainfall amount, seasonality and event size distribution. Larger PPT difference between periods/years resulted in larger legacy impacts, with dry legacies fostering more C sequestration and wet legacies more C release. By analyzing the resource pool (C, N, and H_2O) responses to the simulated dry and wet legacies, we found that the carryover of soil N between periods/years was mainly responsible for the GEP responses while the carryovers of plant biomass, litter and soil organic matter were mainly responsible for the R_e responses. These simulation results suggest that previous PPT conditions can exert substantial legacy impacts on current ecosystem C balance, which should be taken into account

while assessing the response of dryland ecosystem C dynamics to future PPT regime changes.

1 Introduction

Drylands play an important role in global carbon (C) cycle and future C sequestration (Houghton et al., 1999; Asner et al., 2003), as they cover 30–45 % of the earth's land surface (Asner et al., 2003; Reynolds et al., 2007), store about 15 % of the global soil organic carbon (Schlesinger, 1991), and represent 30–35 % of the terrestrial net primary production (Field et al., 1998). Driven by sporadic precipitation (PPT) and nonlinear biological responses, dryland C fluxes are especially variable across time and space (Maestre et al., 2012; Collins et al., 2014), making the prediction of dryland C budgets a challenging task (Jenerette et al., 2012). Moreover, climate models predict that the intra- and inter-annual PPT variability may be further intensified in dryland regions with longer drought durations and more large-sized events (Solomon et al., 2007; Diffenbaugh et al., 2008; Cook and Seager, 2013). Further, sequences of wet years followed by sequences of dry years and vice versa are also increasingly likely (Peters et al., 2012; Sala et al., 2012). Understanding the response of dryland ecosystem C fluxes to PPT variation is, therefore, important to characterizing the global C cycle and predicting how future PPT regime changes will affect dryland C balance.

As a measure of ecosystem C balance, net ecosystem production (NEP) has a value that is positive when an ecosystem accumulates C and negative when an ecosystem loses C. Dryland NEP has been thought to be closely tied to current-year PPT amount, with wetter than average years being a C sink, drier than average years being a C source, and years with average rainfall being C neutral (Flanagan et al., 2002; Hastings et al., 2005). In addition, the precipitation legacy effect, defined as the impact of past PPT conditions on the current structure and functioning of ecosystems (Lauenroth and Sala, 1992; Sala et al., 2012; Monger et al., 2015), has been found to play an important role in shaping the temporal variability of dryland ecosystem C fluxes (Knapp et al., 2002; Heisler and Weltzin, 2006; Sala et al., 2012; Ogle et al., 2015). For example, Hasting et al. (2005) attributed the C sink status of a desert shrub ecosystem in the early spring of 2002 to the above-average rainfall in the late fall of 2001. Scott et al. (2009) and Hamerlynck et al. (2013) found that the cool season (December–April) drought was followed by an unusually large net C loss during the following warm monsoon season (July–September) in semiarid savanna and grassland ecosystems in southwestern US. Moreover, the savanna ecosystem has recently been a net C source and one hypothesized explanation is current respiration of organic C that accumulated in the preceding wetter decade (Scott et al., 2009), but has yet been tested. While these studies reveal the existence of PPT legacy effects on NEP at the seasonal scale, the contribution of PPT legacy to the temporal variability of dryland NEP at interannual and interdecadal time scales has not been quantitatively assessed, mainly because it is methodologically difficult to separate the past and current PPT impacts on C fluxes with observational data (Sala et al., 2012), and there is a general lack of field manipulative experiments to address the PPT legacies at these scales (Reichmann et al., 2013a).

Much of our current understanding of the PPT legacy effects on dryland C fluxes is based on the aboveground net primary production (ANPP). A number of studies have documented that dryland ANPP is not only linearly related to current-year PPT, but also closely related to the PPT amount and seasonality several months to years before (Lauenroth and Sala, 1992; Oesterheld et al., 2001). For example, field studies have found a positive wet legacy effect where ANPP is higher than expected if preceded by a wetter year, or a negative dry legacy effect where ANPP is lower than expected if preceded by a drier year (Jobbagy and Sala, 2000; Oesterheld et al., 2001; Wiegand et al., 2004; Sherry et al., 2008; Sala et al., 2012). Proposed mechanisms explaining such observed PPT legacy effects on ANPP mainly involve the carryover of structural attributes between years. The structural attributes can include leaf and root biomass (Oesterheld et al., 2001), the composition of species differing in rooting depth and phenology (Paruelo et al., 1999; Jobbagy and Sala, 2000; Jenerette et al., 2010), or the density of seeds, tillers and plant individuals (Oesterheld et al., 2001; Yahdjian and Sala, 2006; Reichmann et al., 2013a). Alternatively, production may be lower than expected if proceeded by a wet period (a negative wet legacy effect) or higher than expected if preceded by a dry period (a positive dry legacy effect) (Jenerette et al., 2010). Such PPT legacy effects may be influenced more by biogeochemical effects that influence the resource availability to respond to current PPT (Evans and Burke, 2013; Reichmann et al., 2013b), whereby increased growth in response to a higher PPT can reduce the available nutrients (e.g. nitrogen (N)) for the following period and vice versa. Although various mechanisms have been proposed for the PPT legacy impacts on ANPP, few of them have been rigorously tested and the key underlying mechanisms still remain poorly understood (Sherry et al., 2008; Sala et al., 2012; Monger et al., 2015).

Soil respiration (R_s), as a major component of ecosystem C efflux, has also been found to have lagged responses to PPT variations (Sponseller, 2007; Ma et al., 2012; Cable et al., 2013). This is particularly true at the event scale; after a period of drought, a rainfall event can result in a pulse of CO_2 efflux that may be orders of magnitude larger than that before the event and then decline exponentially for a few days to weeks (Xu et al., 2004; Jenerette et al., 2008; Borken and Matzner, 2009; Cable et al., 2013). At a seasonal scale, Vargas et al. (2010) found no lags between R_s and soil moisture across 13 vegetation types including four grasslands; but Hamerlynck et al. (2013) presented longer-term ecosystem flux data that suggest seasonal drought legacy affects ecosystem respiration (R_e) in a semi-desert grassland in southeastern AZ, US. They posited that the increased C substrate availability resulting from the previous cool-season drought induced plant mortality was responsible for the higher R_e in the following monsoon season. However, very few studies have been devoted to understanding the PPT legacy impacts on dryland respiration at greater than seasonal timescales.

In this study, we conducted simulation experiments with a widely-used dryland ecosystem model, Patch Arid Land Simulator (PALS; Kemp et al., 1997, 2003; Reynolds et al., 2004; Shen et al., 2009), to analyze the PPT legacy effects on ecosystem-level C fluxes including NEP, gross ecosystem production (GEP), and R_e. The PALS model was built on the pulse-reserve concept (Noy-Meir, 1973) and had been used to analyze the impacts of antecedent moisture conditions and the lagged responses of different plant functional types in three North American deserts at the rainfall event scale (Reynolds et al., 2004). We parameterized, calibrated, and evaluated the model based on the long-term eddy covariance measured fluxes at a semidesert ecosystem in southwestern US (Scott et al., 2009) to analyze the PPT legacy effects at interannual and interdecadal scales. Specifically, we aimed to address the following three questions. First, what are the direction and magnitude of ecosystem C flux responses to dry and wet legacies? We expected that the PPT legacy impacts would occur over annual and decadal scales in correspondence to PPT fluctuations at these scales and the dry and wet legacy impacts would differ in direction and magnitude. Second, how are the direction and magnitude of PPT legacy effects related to the PPT characteristics of both the previous and the current year/period? For PPT characteristics, we were not only interested in the annual and seasonal PPT amount but also between-event interval and event size distribution since all these variables are widely-recognized key PPT features to dryland ecosystems. Third, what are the mechanisms responsible for the PPT legacy effects? We assumed that changes in the structural and biogeochemical pools/reserves (C, N, and H_2O) resulting from changes in previous year/period PPT would influence current ecosystem C fluxes as conceptualized in the pulse-reserve framework and implemented in the PALS model.

2 Methods

2.1 Model description

PALS is a process-based ecosystem model that consists of four modules: atmospheric forcing, water cycling and energy budget, plant production and respiration, and soil organic matter (SOM) decomposition and heterotrophic respiration (R_h). The four modules are interactively linked by the cycling of C, N, and H_2O through the atmosphere-plant-soil continuum. The PALS model explicitly considers seven plant functional types (FTs) commonly found in the North American warm deserts: evergreen shrub, deciduous shrub, perennial forb, perennial C_3 and C_4 grasses, and native and exotic C_3 annual grasses (Reynolds et al., 1997; Shen et al., 2009). Since the detailed model structure and mechanistic relationships have been presented in several publications (Kemp et al., 1997, 2003; Reynolds et al., 1997, 2000, 2004; Gao and Reynolds, 2003; Shen et al., 2005, 2008a, b, 2009), here we briefly describe the four modules and refer interested audience to the specific literature.

The atmospheric driving force module reads in data for atmospheric driving variables (e.g. atmospheric [CO_2], N deposition rate, daily maximum and minimum air temperatures, precipitation, relative humidity, and solar radiation), and based on these driving variables, calculates other important variables such as vapor pressure deficit (VPD) that determines stomatal conductance and soil temperature that influences SOM decomposition and soil respiration. Calculations of VPD and soil temperature can be found in Eqs. (2)–(7) in Shen et al. (2005).

The water cycling and energy budget module mainly calculates soil water contents at six layers, the rates of water infiltration into and percolation out of a layer, and water losses via evaporation and transpiration from different layers. Water infiltration and percolation rates of a layer are determined by the effective PPT reaching the soil surface, previous water content, and the water holding capacity as a function of soil texture (Shen et al., 2005). Soil evaporation is determined by soil water availability and energy available in the two top soil layers (10 cm in depth). Water uptake by plants is partitioned among the soil layers according to the proportion of roots in each layer for all plant FTs (Kemp et al., 1997; Shen et al., 2008b). Canopy transpiration is calculated by using the energy budget and the canopy stomatal resistance (Reynolds et al., 2000; Gao and Reynolds, 2003).

The plant production and respiration module mainly simulates phenology, primary production, growth and maintenance respiration, photosynthate allocation, and litterfall of each plant FT. Three major phenophases (i.e. dates of germination, leafing, and dormancy) are determined in PALS based on the observed dates, air temperature, and precipitation (Shen et al., 2009). Primary production for each FT is calculated based on the leaf area, potential net photosynthetic rate, stomatal conductance, leaf N content modifier, and the difference between intercellular and atmospheric [CO_2] (see Eqs. 10–14 in Shen et al., 2005). Photosynthate is allocated to different plant organs (leaf, stem, and root) using fixed allocation ratios after subtracting the maintenance respiration, which is estimated as a function of live biomass, basal respiration rate, and modifiers of temperature and plant water potential (Shen et al., 2008a). Growth respiration is calculated based on the growth yield coefficient and the net photosynthate used for growth (Shen et al., 2008a). Litterfall amount is mainly determined as a function of observed dormancy dates, maximum air temperature and drought conditions (Shen et al., 2008a, 2009).

The SOM decomposition and heterotrophic respiration module simulates the decomposition of metabolic and structural litter material, SOM in active, slow and passive pools, and CO_2 emissions associated with these decomposition processes (Kemp et al., 2003 and Shen et al., 2009). In addition, this module also simulates the dynamics of soil mineral N pool by using N mineralization and atmospheric deposition as the major inputs, and plant N uptake and leaching loss as the major outputs. Among these the N mineralization and plant uptake processes are modeled in more detail while the rates of the other processes are basically assigned with empirical constant values. The N mineralization processes are directly coupled to litter and SOM decomposition processes and are calculated as a product of the C flow rates and the C/N ratio of the corresponding litter or SOM pools (Parton et al., 1993; Kemp et al., 2003). The plant N uptake is a product of water transpiration and N concentration in soil solution (see Eq. 8 in Shen et al., 2008b).

2.2 Model parameterization

For this study, we modified and parameterized PALS to represent an upland mesquite savanna ecosystem in the Santa Rita Experimental Range (SRER; 31.8214° N, 110.8661° W, elevation 1116 m), about 45 km south of Tucson, AZ, USA. Soils at this site are a deep sandy loam (Scott et al., 2009), and the mean groundwater depth likely exceeds 100 m (Barron-Gafford et al., 2013). Precipitation was therefore considered as the only source of water input into the system. Based on the vegetation composition (Scott et al., 2009), there were five major plant FTs included in PALS: shrub (e.g. *Prosopis velutina*), subshrub (e.g. *Isocoma tenuisecta*), C_4 perennial grass (e.g. *Digitaria californica*), perennial forb (e.g. *Ambrosia psilostachya*), and C_3 annual grass, among which the velvet mesquite shrub with average height of ca. 2.5 m accounted for ~ 35 % of the total canopy cover and other FTs (mainly perennial grasses) accounted for ~ 22 % (Scott et al., 2009). Therefore, we derived the site-characteristic parameters for the two major FTs (shrub and perennial grass) from previous studies carried out in SRER, with those for the other FTs being adopted from a generic parameter dataset for the PALS model to be used in the North American warm deserts (Reynolds et al., 2004; Shen et al., 2005). These site-specific parameters mainly included plant-related parameters (e.g. canopy cover, C allocation ratio, rooting distribution ratio, and the initial values of living and dead plant biomass pools) and soil-related parameters (e.g. soil chemical and physical properties, C/N ratios, decomposition rates, and initial values of the litter and SOM pools). The values of these parameters are provided in Supplement Table S1, with cited literature also being listed below the table.

For the climatic variables used to drive the PALS model, we compiled a 30 year meteorological dataset that included daily precipitation (PPT), maximum and minimum air temperatures ($T_{\max}$ and $T_{\min}$), relative humidity (RH), and total solar radiation (S_{rad}) from 1981 to 2010. The $T_{\max}$, $T_{\min}$, RH, and S_{rad} data from 1981–1990 were observations from the Tucson Weather Station (about 50 km north of the mesquite savanna site and lower elevation) and obtained through the Arizona Meteorological Network online

Title Page
Abstract Introduction
Conclusions References
Tables Figures
◀| |▶
◀ ▶
Back Close
Full Screen / Esc
Printer-friendly Version
Interactive Discussion

data access (AZMET: http://ag.arizona.edu/azmet). The remaining 20 years (1991–2010) of $T_{\max}$, $T_{\min}$, RH and S_{rad} data were observations from the Kendall Weather Station (about 85 km east of the mesquite savanna site and slightly higher elevation) and obtained through the Southwest Watershed Research Center (SWRC) online data access (http://www.tucson.ars.ag.gov/dap/). The 30 year PPT data were observations from the Santa Rita Watershed rain gage #5 (1.5 km from the site) and obtained also from the SWRC online data access. These different sources of meteorological data were adjusted based on the 7 years (2004–2010) of the meteorological data obtained from the AmeriFlux eddy-covariance flux tower at the mesquite savanna site (US-SRM, see Supplement Fig. S1). At last, we used the AZMET and SWRC data from 1981 to 2003 plus the flux tower data from 2004 to 2010 to drive the model.

Since our simulation experiment was based on the manipulations of the 30 year (1981–2010) PPT data, we report the PPT characteristics here in more detail. In the past 30 years, the mean annual PPT amount was 401 mm at the site, slightly greater than the long-term (1937–2007) mean of 377 mm (Scott et al., 2009). Based on the seasonal PPT amount, we distinguished four seasons with their mean PPT being listed in parenthesis: the cool growing season from December to March (cool-GS, 104 mm), the warm dry season from April to June (warm-DS, 27 mm), the warm growing season from July to September (warm-GS, 223 mm), and the cool dry season from October to November (cool-DS, 47 mm). At the site, as in many other dryland regions (Sala et al., 1992; Heisler-White et al., 2008), most rainy days have only light amounts. About 80 % of daily rainfall was < 10 mm, with medium- to large-sized events (10–50 mm) accounting for about 20 % and only 10 events larger than 50 mm in the 30 years. The no-rain-day duration between events (hereafter between-event interval or BEI) was ~ 5 days on average in the warm-GS and ~ 10 days in the cool-GS.

To further assess the degree of dryness/wetness of a particular year or growing season relative to the normal annual or seasonal rainfall, we computed the Standard Precipitation Index (SPI) for the 30 years and the 2 growing seasons of each year using the software SPI_SL-6 (available at http://drought.unl.edu/MonitoringTools), with

SPI ≈ 0 indicating a normal year/season, SPI < 0 a dry year/season, and SPI > 0 a wet year/season. Based on the computed SPI, the 30 years were divided into two periods: a wet period from 1981–1994 with mean annual rainfall of 465 mm and a dry period from 1995 to 2010 with mean annual rainfall of 345 mm (Fig. 1a). The 1995–2010 dry period was dominated by cool-GS drought (Fig. 1b), whereas the warm-GS seemed to be wetter in the 1981–1994 wet period (Fig. 1c). These SPI values were used to analyze the relationships between PPT legacy effect and PPT amount.

2.3 Model calibration and evaluation

After model parameterization, we calibrated the model based on four years (2004–2007) of CO_2 and H_2O flux data monitored using the eddy covariance technique at the savanna site. Detailed descriptions of instrumentation, sensor heights and orientations, and data processing procedures for the eddy covariance data can be found in Scott et al. (2009). During model calibration, we mainly adjusted the parameter values of photosynthate allocation ratios, live biomass death rates, and SOM decomposition rates to achieve a best fit between modeled and observed GEP and R_e. The model performed well in capturing the seasonal variation patterns of actual evapotranspiration (AET), GEP, R_e, and NEP in the four years (Supplement Fig. S2), with faster C exchanges during the warm-GS. At seasonal and annual scales, simulated AET, GEP, and R_e could explain over 90 % of the variations in observed ones (Fig. 2, left panels). Compared to AET, GEP, and R_e, the correlation between simulated and observed NEP was weaker. This was mainly due to the poor match in 2006: the model substantially overestimated GEP during the warm-GS but underestimated R_e during the cool-GS (Supplement Fig. S2). If the data of this year were excluded, the explanative power for annual and seasonal NEP was 52 %. Year 2006 had extreme cool-GS drought with the SPI = −2.09 (Fig. 1b) and rainfall of 35 mm – less than half of those in the other three years. This cool-GS drought may have caused increased plant mortality similar to that reported for a semi-desert grassland nearby our study site (Scott et al., 2010; Hamerlynck et al., 2013). We suspect that the model failed to capture such extreme drought impacts and resulted in the poor performance in 2006, since the empirical relations describing plant mortality and climate conditions in PALS account for more normal, rather than extreme, conditions. This is appropriate for our study as we are examining non-extreme influences of legacies.

The model performance was further evaluated by assessing the degree of correlation between the PALS-simulated and flux-tower-measured C and H_2O fluxes from 2008 through 2010, which were not used for model calibration. The coefficients of determination (R^2), which describe the proportion of the variance in measured data explained by the model, were all larger than 0.8 at the seasonal and annual scales (Fig. 2, right panels). Model performance is typically considered to be acceptable with R^2 value > 0.5 (Moriasi et al., 2007). These evaluation results indicate that the model was capable of capturing the temporal variability of observed fluxes at seasonal and annual scales. Since our goal was to use an empirically plausible model to understand long-term temporal variations of ecosystem fluxes, we therefore consider the overall model performance acceptable.

2.4 Simulation experiments

We designed two sets of simulation experiments to examine the interdecadal and interannual PPT legacy effects. To analyze the interdecadal legacy effects, we first changed the PPT of the 14 year previous period (1981–1994) by 0, ±10, ±30, ±50 and ±80 % (multipliers of existing daily PPT amounts in the record) while keeping the 16 year current-period (1995–2010) PPT unchanged. After these manipulations, the average PPT of the previous period ranged from 93 mm corresponding to the 80 % of decrease to 837 mm corresponding to the 80 % of increase. This design detects how changes in previous-period PPT influence the current-period C fluxes and the associated C pool dynamics. On top of each previous period PPT manipulation level, we further changed the current-period PPT by 0, ±10, ±30, ±50, and ±80 %, which resulted in the average current-period PPT varying from 69 to 621 mm. This design detects how changes in the current-period PPT influence the legacies resulting from changes in the previous-period PPT. As a result, we made 73 simulation runs corresponding to the 73 combinations of the above previous- and current-period PPT manipulations (9 previous PPT levels times 8 current PPT levels plus 1 baseline run).

To analyze the interannual legacy, we changed the PPT of each individual year by ±30 % while keeping the PPT of the subsequent years unchanged. This design resulted in 54 simulation runs (27 years from 1981–2007 times 2 PPT manipulation levels) and illustrates the effects of changes in the PPT of the previous one year on the C fluxes and resource pools of the current year(s). After a 30 % of PPT change, annual PPT ranged from 162 to 925 mm in the 27 years, which was large enough to cover the PPT interannual variation at the study site. Another consideration of using 30 % as the PPT manipulation level was that future projected annual PPT variation in dryland regions will be −30 to +25 % (Bates et al., 2008; Maestre et al., 2012).

2.5 Data analysis

Legacy effect was quantified as the C flux (or resource pool size) of the current-period/year after PPT changes in the previous-period/year minus that without PPT changes in the previous-period yr^{-1}. As an example, the following equation calculates the legacy effect of increasing the previous-period PPT by 30 % on the current-period NEP:

$$\mathrm{Legacy}_{\mathrm{NEP}} = \mathrm{NEP}^{\mathrm{CP}}_{\mathrm{PPT}+30\,\%} - \mathrm{NEP}^{\mathrm{CP}}_{\mathrm{PPT}+0\,\%} \tag{1}$$

where $\mathrm{NEP}^{\mathrm{CP}}_{\mathrm{PPT}+30\,\%}$ is the cumulative NEP throughout the current period (1995–2010) under a 30 % of previous-period (1981–1994) PPT increase; $\mathrm{NEP}^{\mathrm{CP}}_{\mathrm{PPT}+0\,\%}$ is the cumulative NEP throughout the current period with no previous-period PPT change. This method directly quantifies whether changes in PPT of the previous period will impose a positive, negative, or no legacy effect on the C fluxes (or resource pools) of the current period. For simplicity, hereafter we refer to the legacy effect resulting from the decreased previous-period/year PPT as the dry legacy and that resulting from the increased previous-period/year PPT as the wet legacy. Spearman correlation analysis was used to detect the relationships between legacy effects and PPT characteristics, including SPI, BEI, and the number of large (≥ 10 mm) vs. small (< 10 mm) events at yearly and seasonal scales. The correlation analysis was performed in SPSS 16.0 (Chicago, IL, USA).

3 Results

3.1 Interdecadal legacy

Changes in the PPT of the previous period (1981–1994) imposed obvious legacy impacts on the C fluxes of the current period (1995–2010). The direction of the simulated interdecadal dry and wet legacies on GEP and R_e was dependent upon the direction of both the previous- and current-period PPT changes. When the current-period PPT was reduced (Fig. 3, left panels), the simulated dry legacies imposed mostly positive impacts on the current-period GEP (Fig. 3a) but negative impacts on R_e (Fig. 3c); whereas wet legacies imposed mostly negative impacts on the current-period GEP (Fig. 3a) but positive impacts on R_e (Fig. 3c). When the current-period PPT was enhanced (Fig. 3, right panel), both the dry and wet legacies imposed mostly positive impacts on GEP and R_e (Fig. 3b and d). Regardless of current-period PPT changes, NEP always responded positively to the dry legacies but negatively to the wet legacies (Fig. 3e and f), indicating that the direction of NEP responses to the PPT legacies was predominantly determined by the direction of the previous-period PPT changes.

The simulated absolute magnitude of the PPT legacies on ecosystem C fluxes (i.e. GEP, R_e, and NEP) generally increased with the absolute magnitude of changes in the previous-period PPT (Figs. 3 and 4). Increasing the current-period PPT generally amplified the legacy effects compared to decreasing the current-period PPT (comparing the left to the right panels of Fig. 3). The magnitude of the PPT legacies was also significantly correlated with the PPT difference between the previous and current period (Δ PPT, equals to the current-period PPT minus the previous-period PPT; Fig. 4). If the previous period was wetter than the current period (i.e. $\Delta\,\mathrm{PPT} < 0$ or a wet-to-dry period transition), the legacy effect on R_e was negatively related with $\Delta\,\mathrm{PPT}$ (Fig. 4c) but that on NEP was positively related with $\Delta\,\mathrm{PPT}$ (Fig. 4e), indicating more current-period C release after a wetter previous period. In contrast, if the previous period was drier than the current period (i.e. $\Delta\,\mathrm{PPT} > 0$ or a dry-to-wet period transition), the correlations were all positive for GEP, R_e and NEP (Fig. 4, right panels), indicating more current period C sequestration after a drier previous period.

The resource pool dynamics were also shaped by the alterations in the previous- and current-period PPTs. We only showed the 30 % decrease and increase in the previous- and current-period PPT (i.e. 4 out of 72 pairs of PPT change combinations) as representative examples in Fig. 5, because the major response patterns for the other paired combinations were similar. The duration of the PPT legacy impacts generally lasted for about 6–8 years for plant biomass, litter mass and soil water content (SWC), but much longer for soil organic matter (SOM) and soil mineral N ($\mathrm{N_{soil}}$) (Fig. 5). Based on the resource pool responses in the early 1–2 years (i.e. 1995 and 1996) of the current period, the dry legacies imposed negative impacts on biomass, litter and SOM (Fig. 5a–f), but positive impacts on $\mathrm{N_{soil}}$ (Fig. 5g and h). Contrastingly, the wet legacies imposed positive impacts on biomass, litter and SOM (Fig. 5a–f), but negative impacts on $\mathrm{N_{soil}}$ (Fig. 5g and h). Similar to the influences on C fluxes, increasing the current-period PPT (Fig. 5, right panels) amplified the legacy impacts on biomass and litter (Fig. 5a–d), and hastened the recovery rates of SOM and $\mathrm{N_{soil}}$ to their baseline levels (Fig. 5e–h).

3.2 Interannual legacy

At the interannual scale, a 30 % decrease or increase in the PPT of one previous year could cause the legacy impacts for 2–12 following years (Fig. 6a and b). The simulated dry legacies had mostly positive impacts on GEP (Fig. 6c) and NEP (Fig. 6g) but negative impacts on R_e (Fig. 6e). Conversely, the simulated wet legacies imposed mostly negative impacts on GEP (Fig. 6d) and NEP (Fig. 6h) but positive impacts on R_e

(Fig. 6f). However, both the direction and magnitude of the simulated dry and wet legacies were very variable and idiosyncratic at this timescale, depending on the C fluxes of interest and the PPT conditions of specific years. The correlation analysis showed that the simulated dry and wet legacies on NEP were only significantly related with the previous-year PPT conditions including annual and warm-GS SPI, BEI, and number of large events (NE > 10 mm; $P < 0.05$; Table 1), but not the current-year PPT conditions (Table 1). With respect to GEP and R_e responses, only the wet legacies were found to be significantly correlated with some of these PPT variables ($P < 0.05$; Table 1). Further examining the correlation between the PPT legacy effects and the PPT difference between two consecutive years (i.e. Δ PPT = current-year PPT minus previous-year PPT), we found that only R_e and NEP responses were significantly correlated with Δ PPT if Δ PPT < 0 (i.e. under a wet-to-dry year transition; Fig. 7c and e).

To analyze the interannual PPT legacy impacts on the dynamics of resource pools (i.e. biomass, litter, SOM, N_{soil}, and SWC), two wet years (1983 and 1994) with positive SPI and two dry years (1986 and 1995) with negative SPI (see Fig. 1a) were chosen as examples. The simulated dry legacies had negative impacts on biomass, litter and SOM, but positive impacts on N_{soil} and SWC in the first current year (Fig. 8). In contrast, wet legacies imposed just the opposite direction of impacts on the five resource pools. The simulated PPT legacy impacts on the resource pools could also last for several years, and the direction and magnitude of the legacy impacts in the following years could differ from those in the first year as described above. For example, increasing the PPT of 1995 by 30 % caused a positive legacy impact on the biomass of the first following year (i.e. 1996) but it became negative in the latter following years (e.g. in 1998; Fig. 8b), further indicating that current-year PPT conditions could influence the direction and magnitude of the previous-year PPT legacies.

4 Discussion

4.1 Direction and magnitude of the simulated PPT legacies

Through this simulation analysis, we demonstrated that previous PPT could impose substantial legacy impacts on current ecosystem C fluxes at interannual and interdecadal timescales. A major finding was that the direction and magnitude of the simulated PPT legacies on NEP were predominantly determined by the previous PPT changes. However, the legacy impacts on the two processes (GEP and R_e) determining NEP ($\text{NEP} = \text{GEP} - R_e$) were largely influenced by both the previous and current PPT changes (Figs. 3a–d and 6c–f). The main reason was that alterations in current PPT influenced GEP and R_e in the same direction (e.g. increasing current PPT stimulated both GEP and R_e) while alterations in previous PPT influenced GEP and R_e in the opposite direction (Figs. 3a–d and 6c–f). These simulation results imply that the direction of the PPT legacy impacts on NEP can be inferred from previous PPT conditions: a previous drier condition may foster more C sequestration in a current wet period/year and a previous wetter condition may cause more C release in a current dry period/year.

Based on the eddy covariance measured NEP, Scott et al. (2009) found that the mesquite savanna ecosystem was a net CO_2 source during the four below-average-rainfall years from 2004 through 2007. They ascribed the net release of C by the system to the cool-GS drought, but also suspected that the system was likely "burning off" much of the C sequestered during the previous wet period (∼ 1975–1995) (Scott et al., 2009). Our simulation results of the positive wet legacy effects on SOM and negative effects on NEP (Fig. 4c and e) support this hypothesis that the accumulated SOM during the previous-wet period (Fig. 5e and f) contributed to the C released during the current dry period. We also found that larger between-period/year PPT difference could result in larger legacy effects (Figs. 4 and 7), which is in agreement with what have been found in some field studies. For example, the magnitude of drought legacy on ANPP is proportional to the severity of the drought (Yahdjian and Sala, 2006; Swemmer et al., 2007), and dry- or wet-year legacies on ANPP are linearly related to the PPT difference between years (Sala et al., 2012; Reichmann et al., 2013a). Our simulation analysis detected that not only annual PPT amount but also finer scale PPT characteristics such as GS-rainfall, BEI, and event size could be important in determining the interannual-scale PPT legacy effects (Table 1). These simulation results suggest that PPT legacies may play an more important role in shaping the temporal variability of dryland ecosystem C fluxes under the projected increase in future PPT variability (Solomon et al., 2007; Cook and Seager, 2013).

Dryland ecosystems are commonly thought to be a C sink in wet years, a C source in dry years, and C neutral in normal years (Flanagan et al., 2002; Hastings et al., 2005). While recent studies have shown the importance of growing season length (Xu and Baldocchi, 2004; Ma et al., 2007), seasonal drought (Scott et al., 2009, 2010; Hamerlynck et al., 2013), and other factors such as temperature and vegetation composition (Hui et al., 2003; Hamerlynck et al., 2010; Barron-Gafford et al., 2012; Scott et al., 2014), our simulation results indicate PPT legacies may also have important consequences to ecosystem C dynamics. For example, PPT was wetter than normal in 1987 with the SPI of 1.21 but with the NEP of $-85\,\mathrm{g\,C\,m^{-2}\,yr^{-1}}$ (a C source), due to the negative wet legacy impacts on NEP several previous wet years before (see Fig. 6h). PPT was nearly normal in 2008 with the SPI of 0.09 but with the simulated NEP of $79.6\,\mathrm{g\,C\,m^{-2}\,yr^{-1}}$ and the observed NEP of $69.2\,\mathrm{g\,C\,m^{-2}\,yr^{-1}}$ (a C sink), again due to the positive dry legacy impacts on NEP from several previous dry years (see Fig. 6g). In a recent analysis on 14 years (1997–2011) of eddy covariance measurements, Zielis et al. (2014) reported that inclusion of previous year's weather (PPT and temperature) into the linear predicting models for NEP increased the explained variance to 53 % compared to 20 % without accounting for previous year's weather, indicating that previous year's weather also played an important role in the Switzerland subalpine spruce forest. Although we compared some response patterns generated from this simulation study with those derived from field observations, there exists no field study that, to our knowledge, is comparable to our simulation experiment to allow us conducting a direct comparison between the simulated and observed responses. The simulation experimental design of this study may provide helpful insights into designing field manipulative experiments to further test the modeled patterns.

4.2 Potential mechanisms of the modeled PPT legacies

There are three basic mechanisms explaining why PPT legacy impacts can occur in the model system like PALS. First, the rate of C fluxes is a function of not only various influential factors (e.g. PPT and temperature) but also the pool size itself. For example, soil heterotrophic CO_2 efflux (R_h) rate is a product of the decomposition coefficient, the size of the SOM pool, and two scalar functions accounting for temperature and moisture influences (Kemp et al., 2003; Shen et al., 2009). Therefore, the altered SOM pool size from previous PPT changes can affect current R_h. Second, different C pools have different turnover rates. If the resources (e.g. water, biomass and SOM) produced in a previous legacy year were not completely lost from the pool/reserve due to slower turnover rate, the resources may be carried over to the current year and influence the C fluxes as explained in the first mechanism. For example, SOM pools in the model have relatively slower turnover rates than biomass pools (Shen et al., 2005, 2008b), thus resulting in the longer-lasting legacy impacts on SOM than on biomass or litter pools (Figs. 5 and 8). Third, the C, N and H_2O cycling processes are closely coupled in the PALS model. Carried-over resources (e.g. C and N) can therefore interact with current PPT conditions to influence the responses of current fluxes. Based on these general model mechanisms, below we discuss more specifically on the major responsive patterns and the responsible biogeochemical carryovers.

An intuitive first explanation for the simulated wet legacies would be the carryover of water. However, in most cases soil water carryover did not occur because the wet and dry legacies on SWC were mostly negative or close to zero at the beginning of the current period/year (Figs. 5i, j and 8i, j). Soil water carryover was therefore not the major contributor to the modeled PPT legacy effects at interdecadal and interannual scales. This simulation result corroborates with those of field studies that carryover of water across long temporal scale is rare in dryland ecosystems, because the rainy growing seasons or wet years are often separated by dry dormant seasons or dry years resulting in short residence time of water in the system (Oesterheld et al., 2001; Reichmann et al., 2013a; Scott et al., 2014). However, it is noted here that the carryover of soil water might be possible at finer temporal scales. For example, Raz-Yaseef et al. (2012) reported that water from large storms could infiltrate into deep soil layers, be stored there for longer periods of time and carried over across seasons/months (also see Wiegand et al., 2004). Thus, carryover of stored soil water should be considered as one of the potential mechanisms while addressing the PPT legacy effects at seasonal or event scales.

The carryover of soil N (N_{soil}) is mainly responsible for the modeled GEP responses. In the PALS model, the photosynthetic rate is linearly related to N availability if plant N demand is not fulfilled (Reynolds et al., 2004; Shen et al., 2005). The enhanced N_{soil} as dry legacies (Figs. 5g, h and 8g, h) therefore resulted in the mostly positive responses of GEP (Figs. 3a, b and 6c). Conversely, the reduced N_{soil} by wet legacies (Figs. 5g, h and 8g, h) resulted in the mostly negative responses of GEP (Figs. 3a, b and 6d). The simulated dry legacies increased N_{soil} mainly by decreasing PPT suppressed plant growth and therefore N uptake. This is consistent with many field measurements that N_{soil} accumulates under drought conditions (Reynolds et al., 1999; Yahdjian et al., 2006; de Vries et al., 2012; Evans and Burke, 2013; Reichmann et al., 2013b). Also similar to our simulation results, field studies found that N uptake increases and N_{soil} decreases under wet conditions in dryland ecosystems (McCulley et al., 2009; Reichmann et al., 2013b). The N enhancement as dry legacies also explains why the simulated dry legacy impacts on NEP were positive (Figs. 3e, f and 6g), particularly under the circumstance of the dry-to-wet period/year transition (Figs. 4e and 7e). The N_{soil} carried over from the previous dry period/year and the current wetter conditions ameliorated both the N and H_2O limitations on GEP, therefore resulted in more C sequestration in the current period/year.

The carryover of organic matter (biomass, litter and SOM) is mainly responsible for the modeled R_e responses. In the PALS model, the autotrophic (R_a) and heterotrophic

(R_h) respiration rates are linearly related to the size of biomass, litter and SOM pools (Kemp et al., 2003; Shen et al., 2008a, 2009). The previous wet condition stimulated biomass, litter and SOM accumulation (Figs. 5 and 8) therefore resulted in the mostly positive wet legacy impacts on R_e (Figs. 3c, d and 6f). Conversely, the dry legacy decreased these pools (Figs. 5 and 8) and therefore resulted in the mostly negative dry legacy impacts on R_e (Figs. 3c, d and 6e). Some field studies suggest that the labile C resulting from litter decomposition in a dry season may stimulate R_h in the following wet season (Jenerette et al., 2008; Scott et al., 2009; Ma et al., 2012), i.e. the dry-season had a positive legacy impact on the labile C pool and R_h, which is contrary to our simulation result that dry legacies are mostly negative on SOM and R_h. This is mainly because the labile soil C pool in the PALS model only accounts for $\sim 3\,\%$ of the total SOM and has a very short residence time (1.7 year; see Supplement Table S1); small amount of seasonal labile C carryover therefore may not exert obvious legacy impacts on SOM and R_h across interannual and interdecadal scales. These results imply that the PPT legacy effects differs in direction and magnitude, depending on the type of C fluxes under consideration, the type of legacies (i.e. dry vs. wet), and the temporal scale of analysis.

5 Conclusions

Through this simulation analysis, we learned that: (i) previous PPT conditions can impose substantial legacy impacts on the C balance of dryland ecosystems, with dry legacies fostering more current C sequestration and wet legacies causing more current C release, (ii) the responses of ecosystem C fluxes to the simulated dry and wet legacies are mostly opposite in direction and asymmetrical in magnitude, with dry legacies being greater for GEP than for R_e and wet legacies being greater for R_e than for GEP, (iii) the carryover of N_{soil} is mainly responsible for the GEP responses, and the carryovers of biomass, litter and SOM are mainly responsible for the R_e responses, and (iv) the simulated PPT legacy effects can last for several years even with one-year

PPT change and therefore the direction and magnitude of PPT legacy effects are less predictable at interannual than at interdecadal scale.

Our simulation results imply that with the predicted decreasing trends in future PPT amount (Seager et al., 2007; Solomon et al., 2007), dryland ecosystems in southwestern US may emit more C that was sequestered in the past into the atmosphere. With the projected more extreme and variable PPT regime (Seager et al., 2007; Solomon et al., 2007; Diffenbaugh et al., 2008), the temporal variability of ecosystem C fluxes may be further intensified in the region due to the increasing PPT variability and the associated legacy impacts. While this simulation analysis mainly addressed the PPT legacy impacts on dryland ecosystem C fluxes from a biogeochemical perspective, structural shifts in vegetation composition such as woody plant encroachment (Potts et al., 2008; Scott et al., 2014) exotic species invasion (Hamerlynck et al., 2010; Scott et al., 2010), and changes in microbial communities (de Vries et al., 2012; Evans and Wallenstein, 2012; Collins et al., 2014), may also interact with the biogeochemical processes to shape the PPT legacy effects on the temporal variability of dryland C fluxes. Future studies incorporating both the structural and biogeochemical aspects and involving multiple temporal scales are needed in order to achieve a more comprehensive understanding of the PPT legacy effects on dryland ecosystem C dynamics.

The Supplement related to this article is available online at doi:10.5194/bgd-12-9613-2015-supplement.

Acknowledgements. We thank the USDA-Agricultural Research Service (ARS), Southwest Watershed Research Center (SWRC) and the Arizona Meteorological Network (AZMET) for making their meteorological data open to access. W. Shen acknowledges the financial supports from the Natural Science Foundation of China (31 130 011, 31 425 005 and 31 290 222), the Major State Basic Research Development Program (973 Planning Program 2011CB403206), and the Natural Science Foundation of Guangdong Province, China (S201 202 0011084). Partial funding for the Santa Rita Mesquite Savanna eddy covariance site is provided by the US Department of Energy AmeriFlux Office (grant DE-AC02-05CH11231).

References

Asner, G. P., Archer, S., Hughes, R. F., Ansley, R. J., and Wessman, C. A.: Net changes in regional woody vegetation cover and carbon storage in Texas drylands, 1937–1999, Glob. Change Biol., 9, 316–335, 2003.

Barron-Gafford, G. A., Scott, R. L., Jenerette, G. D., Hamerlynck, E. P., and Huxman, T. E.: Temperature and precipitation controls over leaf- and ecosystem-level CO_2 flux along a woody plant encroachment gradient, Glob. Change Biol., 18, 1389–1400, 2012.

Barron-Gafford, G. A., Scott, R. L., Jenerette, G. D., Hamerlynck, E. P., and Huxman, T. E.: Landscape and environmental controls over leaf and ecosystem carbon dioxide fluxes under woody plant expansion, J. Ecol., 101, 1471–1483, 2013.

Bates, B. C., Kundzewicz, Z. W., Wu, S., and Palutikof, J. P. (Eds.): Climate Change and Water, Technical Paper of the Intergovernmental Panel on Climate Change, IPCC Secretariat, Genenva, 2008.

Borken, W. and Matzner, E.: Reappraisal of drying and wetting effects on C and N mineralization and fluxes in soils, Glob. Change Biol., 15, 808–824, 2009.

Cable, J. M., Ogle, K., Barron-Gafford, G. A., Bentley, L. P., Cable, W. L., Scott, R. L., Williams, D. G., and Huxman, T. E.: Antecedent conditions influence soil respiration differences in shrub and grass patches, Ecosystems, 16, 1230–1247, 2013.

Collins, S. L., Belnap, J., Grimm, N. B., Rudgers, J. A., Dahm, C. N., D'Odorico, P., Litvak, M., Natvig, D. O., Peters, D. C., Pockman, W. T., Sinsabaugh, R. L., and Wolf, B. O.: A multiscale, hierarchical model of pulse dynamics in arid-land ecosystems, Annu. Rev. Ecol. Evol. S., 45, 397–419, 2014.

Cook, B. I. and Seager, R.: The response of the North American Monsoon to increased greenhouse gas forcing, J. Geophys. Res.-Atmos., 118, 1690–1699, 2013.

de Vries, F. T., Liiri, M. E., Bjornlund, L., Setala, H. M., Christensen, S., and Bardgett, R. D.: Legacy effects of drought on plant growth and the soil food web, Oecologia, 170, 821–833, 2012.

Diffenbaugh, N. S., Giorgi, F., and Pal, J. S.: Climate change hotspots in the United States, Geophys. Res. Lett., 35, l16709, doi:10.1029/2008GL035075, 2008.

Evans, S. E. and Burke, I. C.: Carbon and nitrogen decoupling under an 11 year drought in the shortgrass steppe, Ecosystems, 16, 20–33, 2013.

Evans, S. E. and Wallenstein, M. D.: Soil microbial community response to drying and rewetting stress: does historical precipitation regime matter?, Biogeochemistry, 109, 101–116, 2012.

Field, C. B., Behrenfeld, M. J., Randerson, J. T., and Falkowski, P.: Primary production of the biosphere: integrating terrestrial and oceanic components, Science, 281, 237–240, 1998.

Flanagan, L. B., Wever, L. A., and Carlson, P. J.: Seasonal and interannual variation in carbon dioxide exchange and carbon balance in a northern temperate grassland, Glob. Change Biol., 8, 599–615, 2002.

Gao, Q. and Reynolds, J. F.: Historical shrub-grass transitions in the northern Chihuahuan Desert: modeling the effects of shifting rainfall seasonality and event size over a landscape gradient, Glob. Change Biol., 9, 1475–1493, 2003.

Hamerlynck, E. P., Scott, R. L., Moran, M. S., Keefer, T. O., and Huxman, T. E.: Growing season ecosystem and leaf-level gas exchange of an exotic and native semiarid bunchgrass, Oecologia, 163, 561–570, 2010.

Hamerlynck, E. P., Scott, R. L., and Barron-Gafford, G. A.: Consequences of cool-season drought-induced plant mortality to Chihuahuan Desert grassland ecosystem and soil respiration dynamics, Ecosystems, 16, 1178–1191, 2013.

Hastings, S. J., Oechel, W. C., and Muhlia-Melo, A.: Diurnal, seasonal and annual variation in the net ecosystem CO_2 exchange of a desert shrub community (Sarcocaulescent) in Baja California, Mexico, Glob. Change Biol., 11, 927–939, 2005.

Heisler, J. L. and Weltzin, J. F.: Variability matters: towards a perspective on the influence of precipitation on terrestrial ecosystems, New Phytol., 172, 189–192, 2006.

Heisler-White, J. L., Knapp, A. K., and Kelly, E. F.: Increasing precipitation event size increases aboveground net primary productivity in a semi-arid grassland, Oecologia, 158, 129–140, 2008.

Houghton, R. A., Hackler, J. L., and Lawrence, K. T.: The US carbon budget: contributions from land-use change, Science, 285, 574–578, 1999.

Hui, D. F., Luo, Y. Q., and Katul, G.: Partitioning interannual variability in net ecosystem exchange into climatic variability and functional change, Tree Physiol., 23, 433–442, 2003.

Jenerette, G. D., Scott, R. L., and Huxman, T. E.: Whole ecosystem metabolic pulses following precipitation events, Funct. Ecol., 22, 924–930, 2008.

Jenerette, G. D., Scott, R. L., and Huete, A. R.: Functional differences between summer and winter season rain assessed with MODIS-derived phenology in a semi-arid region, J. Veg. Sci., 21, 16–30, 2010.

Jenerette, G. D., Barron-Gafford, G. A., Guswa, A. J., McDonnell, J. J., and Villegas, J. C.: Organization of complexity in water limited ecohydrology, Ecohydrology, 5, 184–199, 2012.

Jobbagy, E. G. and Sala, O. E.: Controls of grass and shrub aboveground production in the Patagonian steppe, Ecol. Appl., 10, 541–549, 2000.

Kemp, P. R., Reynolds, J. F., Pachepsky, Y., and Chen, J. L.: A comparative modeling study of soil water dynamics in a desert ecosystem, Water Resour. Res., 33, 73–90, 1997.

Kemp, P. R., Reynolds, J. F., Virginia, R. A., and Whitford, W. G.: Decomposition of leaf and root litter of Chihuahuan desert shrubs: effects of three years of summer drought, J. Arid Environ., 53, 21–39, 2003.

Knapp, A. K., Fay, P. A., Blair, J. M., Collins, S. L., Smith, M. D., Carlisle, J. D., Harper, C. W., Danner, B. T., Lett, M. S., and McCarron, J. K.: Rainfall variability, carbon cycling, and plant species diversity in a mesic grassland, Science, 298, 2202–2205, 2002.

Lauenroth, W. K. and Sala, O. E.: Long-term forage production of North-American shortgrass steppe, Ecol. Appl., 2, 397–403, 1992.

Ma, S. Y., Baldocchi, D. D., Xu, L. K., and Hehn, T.: Inter-annual variability in carbon dioxide exchange of an oak/grass savanna and open grassland in California, Agr. Forest Meteorol., 147, 157–171, 2007.

Ma, S. Y., Baldocchi, D. D., Hatala, J. A., Detto, M., and Yuste, J. C.: Are rain-induced ecosystem respiration pulses enhanced by legacies of antecedent photodegradation in semi-arid environments?, Agr. Forest Meteorol., 154, 203–213, 2012.

Maestre, F. T., Salguero-Gomez, R., and Quero, J. L.: It is getting hotter in here: determining and projecting the impacts of global environmental change on drylands Introduction, Philos. T. R. Soc. B, 367, 3062–3075, 2012.

McCulley, R. L., Burke, I. C., and Lauenroth, W. K.: Conservation of nitrogen increases with precipitation across a major grassland gradient in the Central Great Plains of North America, Oecologia, 159, 571–581, 2009.

Monger, C., Sala, O. E., Duniway, M. C., Goldfus, H., Meir, I. A., Poch, R. M., Throop, H. L., and Vivoni, E. R.: Legacy effects in linked ecological-soil-geomorphic systems of drylands, Front. Ecol. Environ., 13, 13–19, 2015.

Moriasi, D. N., Arnold, J. G., Van Liew, M. W., Bingner, R. L., Harmel, R. D., and Veith, T. L.: Model evaluation guidelines for systematic quantification of accuracy in watershed simulations, T. Asabe, 50, 885–900, 2007.

Noy-Meir, I.: Desert ecosystems: environment and producers, Annu. Rev. Ecol. Evol. S., 4, 25–51, 1973.

Oesterheld, M., Loreti, J., Semmartin, M., and Sala, O. E.: Inter-annual variation in primary production of a semi-arid grassland related to previous-year production, J. Veg. Sci., 12, 137–142, 2001.

Ogle, K., Barber, J. J., Barron-Gafford, G. A., Bentley, L. P., Young, J. M., Huxman, T. E., Loik, M. E., and Tissue, D. T.: Quantifying ecological memory in plant and ecosystem processes, Ecol. Lett., 18, 221–235, 2015.

Parton, W. J., Scurlock, J. M. O., Ojima, D. S., Gilmanov, T. G., Scholes, R. J., Schimel, D. S., Kirchner, T., Menaut, J. C., Seastedt, T., Moya, E. G., Kamnalrut, A., and Kinyamario, J. I.: Observations and modeling of biomass and soil organic-matter dynamics for the grassland biome worldwide, Global Biogeochem. Cy., 7, 785–809, 1993.

Paruelo, J. M., Lauenroth, W. K., Burke, I. C., and Sala, O. E.: Grassland precipitation-use efficiency varies across a resource gradient, Ecosystems, 2, 64–68, 1999.

Peters, D. P. C., Yao, J., Sala, O. E., and Anderson, J. P.: Directional climate change and potential reversal of desertification in arid and semiarid ecosystems, Glob. Change Biol., 18, 151–163, 2012.

Potts, D. L., Scott, R. L., Cable, J. M., Huxman, T. E., and Williams, D. G.: Sensitivity of mesquite shrubland CO_2 exchange to precipitation in contrasting landscape settings, Ecology, 89, 2900–2910, 2008.

Raz-Yaseef, N., Yakir, D., Schiller, G., and Cohen, S.: Dynamics of evapotranspiration partitioning in a semi-arid forest as affected by temporal rainfall patterns, Agr. Forest Meteorol., 157, 77–85, 2012.

Reichmann, L. G., Sala, O. E., and Peters, D. P. C.: Precipitation legacies in desert grassland primary production occur through previous-year tiller density, Ecology, 94, 435–443, 2013a.

Reichmann, L. G., Sala, O. E., and Peters, D. P. C.: Water controls on nitrogen transformations and stocks in an arid ecosystem, Ecosphere, 4, 1–17, 2013b.

Reynolds, J. F., Virginia, R. A., and Schlesinger, W. H.: Defining functional types for models of desertification, in: Plant Functional Types: Their Relevance to Ecosystem Properties and Global Change, edited by: Shugart, T. M. and Woodward, F. I., Cambridge University Press, Cambridge, 195–216, 1997.

Reynolds, J. F., Virginia, R. A., Kemp, P. R., de Soyza, A. G., and Tremmel, D. C.: Impact of drought on desert shrubs: effects of seasonality and degree of resource island development, Ecol. Monogr., 69, 69–106, 1999.

Reynolds, J. F., Kemp, P. R., and Tenhunen, J. D.: Effects of long-term rainfall variability on evapotranspiration and soil water distribution in the Chihuahuan Desert: a modeling analysis, Plant Ecol., 150, 145–159, 2000.

Reynolds, J. F., Kemp, P. R., Ogle, K., and Fernandez, R. J.: Modifying the "pulse-reserve" paradigm for deserts of North America: precipitation pulses, soil water, and plant responses, Oecologia, 141, 194–210, 2004.

Reynolds, J. F., Stafford Smith, D. M., Lambin, E. F., Turner, B. L., Mortimore, M., Batterbury, S. P. J., Downing, T. E., Dowlatabadi, H., Fernandez, R. J., Herrick, J. E., Huber-Sannwald, E., Jiang, H., Leemans, R., Lynam, T., Maestre, F. T., Ayarza, M., and Walker, B.: Global desertification: building a science for dryland development, Science, 316, 847–851, 2007.

Sala, O. E., Lauenroth, W. K., and Parton, W. J.: Long-term soil-water dynamics in the shortgrass steppe, Ecology, 73, 1175–1181, 1992.

Sala, O. E., Gherardi, L. A., Reichmann, L., Jobbagy, E., and Peters, D.: Legacies of precipitation fluctuations on primary production: theory and data synthesis, Philos. T. R. Soc. B, 367, 3135–3144, 2012.

Schlesinger, W. H.: Biogeochemistry: an Analysis of Global Change, Academic Press Inc, San Diego, CA, 1991.

Scott, R. L., Jenerette, G. D., Potts, D. L., and Huxman, T. E.: Effects of seasonal drought on net carbon dioxide exchange from a woody-plant-encroached semiarid grassland, J. Geophys. Res.-Biogeosci., 114, G04004, doi:10.1029/2008JG000900, 2009.

Scott, R. L., Hamerlynck, E. P., Jenerette, G. D., Moran, M. S., and Barron-Gafford, G. A.: Carbon dioxide exchange in a semidesert grassland through drought-induced vegetation change, J. Geophys. Res.-Biogeosci., 115, G03026, doi:10.1029/2010JG001348, 2010.

Scott, R. L., Huxman, T. E., Barron-Gafford, G. A., Jenerette, G. D., Young, J. M., and Hamerlynck, E. P.: When vegetation change alters ecosystem water availability, Glob. Change Biol., 20, 2198–2210, 2014.

Seager, R., Ting, M. F., Held, I., Kushnir, Y., Lu, J., Vecchi, G., Huang, H. P., Harnik, N., Leetmaa, A., Lau, N. C., Li, C. H., Velez, J., and Naik, N.: Model projections of an imminent transition to a more arid climate in southwestern North America, Science, 316, 1181–1184, 2007.

Shen, W. J., Wu, J. G., Kemp, P. R., Reynolds, J. F., and Grimm, N. B.: Simulating the dynamics of primary productivity of a Sonoran ecosystem: model parameterization and validation, Ecol. Model., 189, 1–24, 2005.

Shen, W. J., Jenerette, G. D., Hui, D. F., Phillips, R. P., and Ren, H.: Effects of changing precipitation regimes on dryland soil respiration and C pool dynamics at rainfall event, seasonal and interannual scales, J. Geophys. Res.-Biogeosci., 113, G03024, doi:03010.01029/02008JG000685, 2008a.

Shen, W. J., Wu, J. G., Grimm, N. B., and Hope, D.: Effects of urbanization-induced environmental changes on ecosystem functioning in the Phoenix metropolitan region, USA, Ecosystems, 11, 138–155, 2008b.

Shen, W. J., Reynolds, J. F., and Hui, D. F.: Responses of dryland soil respiration and soil carbon pool size to abrupt vs. gradual and individual vs. combined changes in soil temperature, precipitation, and atmospheric [CO_2]: a simulation analysis, Glob. Change Biol., 15, 2274–2294, 2009.

Sherry, R. A., Weng, E. S., Arnone, J. A., Johnson, D. W., Schimel, D. S., Verburg, P. S., Wallace, L. L., and Luo, Y. Q.: Lagged effects of experimental warming and doubled precipitation on annual and seasonal aboveground biomass production in a tallgrass prairie, Glob. Change Biol., 14, 2923–2936, 2008.

Solomon, S., Qin, D., Manning, M., Chen, Z., Marquis, M., Averyt, K. B., Tignor, M., and Miller, H. L. (Eds.): Climate Change 2007: The Physical Science Basis, Cambridge University Press, Cambridge, 2007.

Sponseller, R. A.: Precipitation pulses and soil CO_2 flux in a Sonoran Desert ecosystem, Glob. Change Biol., 13, 426–436, 2007.

Swemmer, A. M., Knapp, A. K., and Snyman, H. A.: Intra-seasonal precipitation patterns and above-ground productivity in three perennial grasslands, J. Ecol., 95, 780–788, 2007.

Vargas, R., Baldocchi, D. D., Allen, M. F., Bahn, M., Black, T. A., Collins, S. L., Yuste, J. C., Hirano, T., Jassal, R. S., Pumpanen, J., and Tang, J. W.: Looking deeper into the soil: biophysical controls and seasonal lags of soil CO_2 production and efflux, Ecol. Appl., 20, 1569–1582, 2010.

Wiegand, T., Snyman, H. A., Kellner, K., and Paruelo, J. M.: Do grasslands have a memory: modeling phytomass production of a semiarid South African grassland, Ecosystems, 7, 243–258, 2004.

Xu, L. K. and Baldocchi, D. D.: Seasonal variation in carbon dioxide exchange over a Mediterranean annual grassland in California, Agr. Forest Meteorol., 123, 79–96, 2004.

Xu, L. K., Baldocchi, D. D., and Tang, J. W.: How soil moisture, rain pulses, and growth alter the response of ecosystem respiration to temperature, Global Biogeochem. Cy., 18, GB4002, doi:10.1029/2004GB002281, 2004.

Yahdjian, L. and Sala, O. E.: Vegetation structure constrains primary production response to water availability in the Patagonian steppe, Ecology, 87, 952–962, 2006.

Yahdjian, L., Sala, O. E., and Austin, A. T.: Differential controls of water input on litter decomposition and nitrogen dynamics in the Patagonian Steppe, Ecosystems, 9, 128–141, 2006.

Zielis, S., Etzold, S., Zweifel, R., Eugster, W., Haeni, M., and Buchmann, N.: NEP of a Swiss subalpine forest is significantly driven not only by current but also by previous year's weather, Biogeosciences, 11, 1627–1635, doi:10.5194/bg-11-1627-2014, 2014.

Table 1. Spearman correlation coefficients between legacy effects and precipitation characteristics at an interannual scale.

Precipitation characteristics	Dry legacy (previous-year PPT −30 %)			Wet legacy (previous-year PPT +30 %)		
	GEP	R_e	NEP	GEP	R_e	NEP
Previous-year PPT characteristics						
Yearly SPI	ns	ns	0.560^{**}	-0.545^{**}	ns	-0.757^{**}
Warm-GS SPI	ns	ns	0.579^{**}	ns	ns	-0.626^{**}
Yearly NE > 10 mm	ns	ns	0.442^{*}	-0.446^{*}	ns	-0.636^{**}
Warm-GS NE > 10 mm	ns	ns	0.445^{*}	ns	ns	-0.575^{**}
Current-year PPT characteristics						
Yearly SPI	ns	ns	ns	-0.482^{*}	-0.467^{*}	ns
Warm-GS SPI	ns	ns	ns	ns	-0.399^{*}	ns
Yearly BEI	ns	ns	ns	0.409^{*}	ns	ns
Yearly NE > 10 mm	ns	ns	ns	-0.394^{*}	ns	ns

Abbreviations: PPT: precipitation; SPI: standard precipitation index; GEP: gross primary production; R_e: ecosystem respiration; NEP: net ecosystem production; GS: growing season; BEI: between-event interval; NE: number of events. * and ** – Correlations are significant at the 0.05 and 0.01 levels (2-tailed), respectively; ns – not significant.

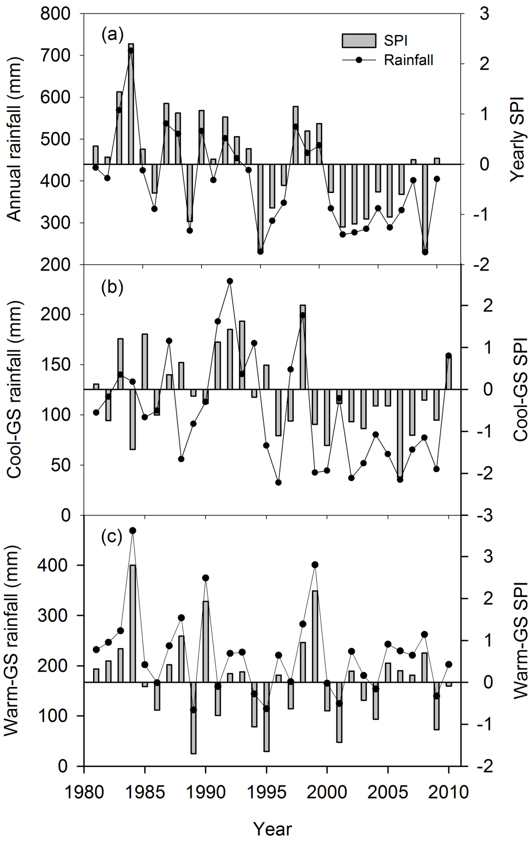

Figure 1. Annual and growing-season rainfall and corresponding standard precipitation index (SPI) in the 30 years (1981–2010) at the Santa Rita Experimental Range (SRER) mesquite savanna site. The cool growing season (cool-GS) is from December through March and warm-GS from July through September. Dots represent annual or seasonal rainfall and bars the corresponding standard precipitation index.

Title Page
Abstract | Introduction
Conclusions | References
Tables | Figures
◀◀ | ▶▶
◀ | ▶
Back | Close
Full Screen / Esc
Printer-friendly Version
Interactive Discussion

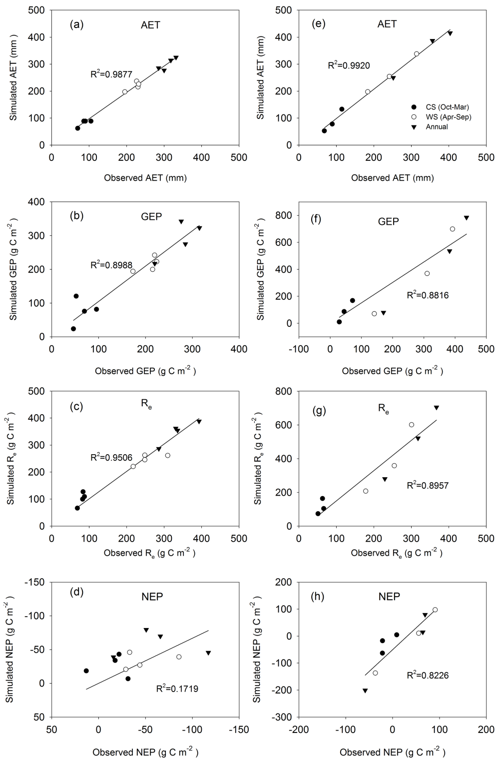

Figure 2. Comparison of the model-simulated water and carbon fluxes with the eddy covariance observed ones at the mesquite savanna site. Left panels show the seasonal and annual fluxes (2004–2007) used for model calibration. Right panels show the seasonal and annual fluxes (2008–2010) used for model validation. R^2 is the coefficient of determination describing the proportion of the variance in measured fluxes explained by the model. CS represents the cool season from October to March and WS the warm season from April to September. AET represents actual evapotranspiration; GEP gross ecosystem production, R_e total ecosystem respiration, and NEP net ecosystem production.

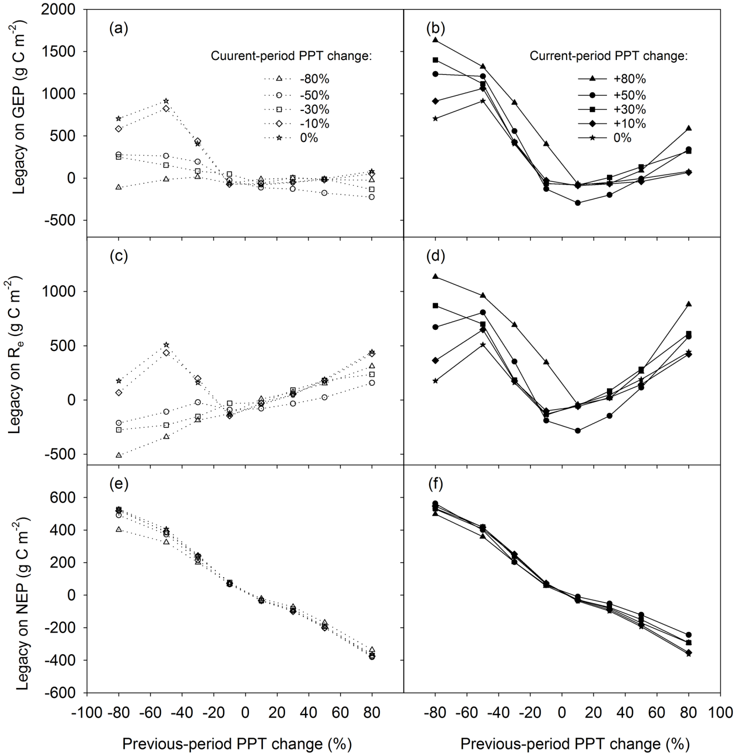

Figure 3. Interdecadal legacy effects of changing the previous-period (1981–1994) precipitation on the cumulative carbon fluxes of the current period (1995–2010). Dashed lines with open symbols represent different levels of decreasing (left panels) the current-period precipitation (PPT). Solid lines with filled symbols represent increasing (right panels) the current-period precipitation.

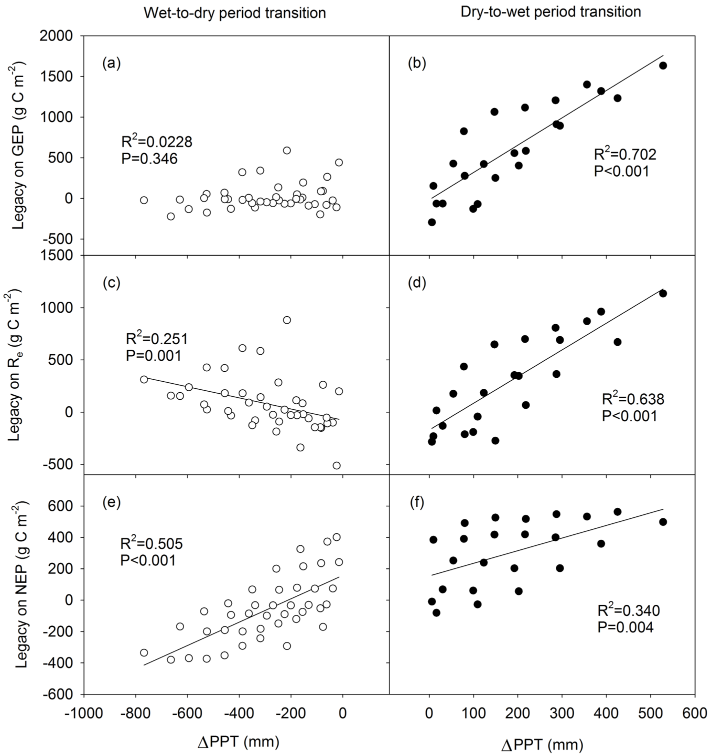

Figure 4. Spearman correlations of interdecadal precipitation legacy effects with the precipitation difference between periods (Δ PPT). Interdecadal Δ PPT is calculated as the mean PPT of the current period (1995–2010) minus that of the previous period (1981–1994). Sample size is 41 for the wet-to-dry period transition (left panels) and 23 for the dry-to-wet period transition (right panels). GEP represents gross ecosystem production, R_e ecosystem respiration, and NEP net ecosystem production. R^2 is the coefficient of determination and P is probability.

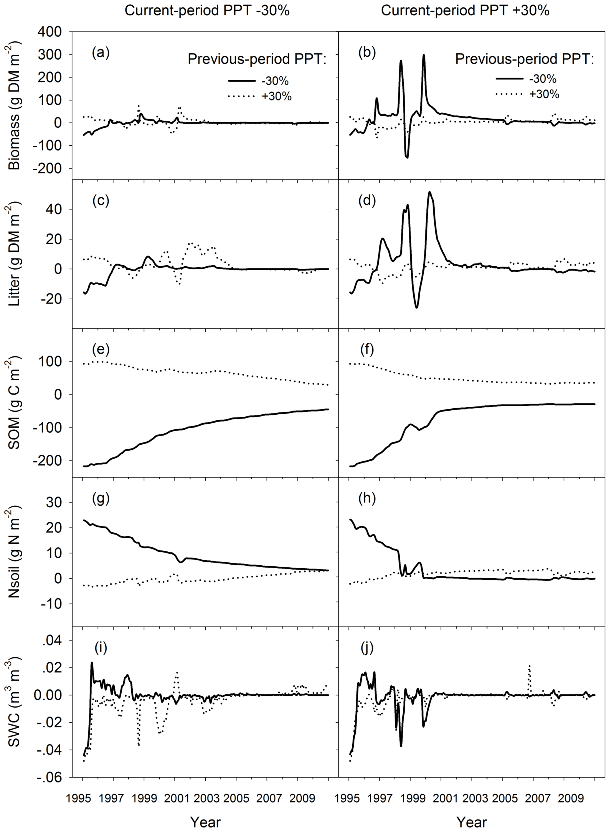

Figure 5. Interdecadal precipitation legacy effects on the resource pool dynamics. Left panels show the resource pool responses under a 30 % of decrease while right panels show those under a 30 % of increase in the precipitation (PPT) of the current period from 1995–2010. Dashed lines represent a 30 % of decrease while solid lines represent a 30 % of increase in the precipitation of the previous period from 1981–1994. SOM represents soil organic matter, N_{soil} soil mineral nitrogen, and SWC soil water content.

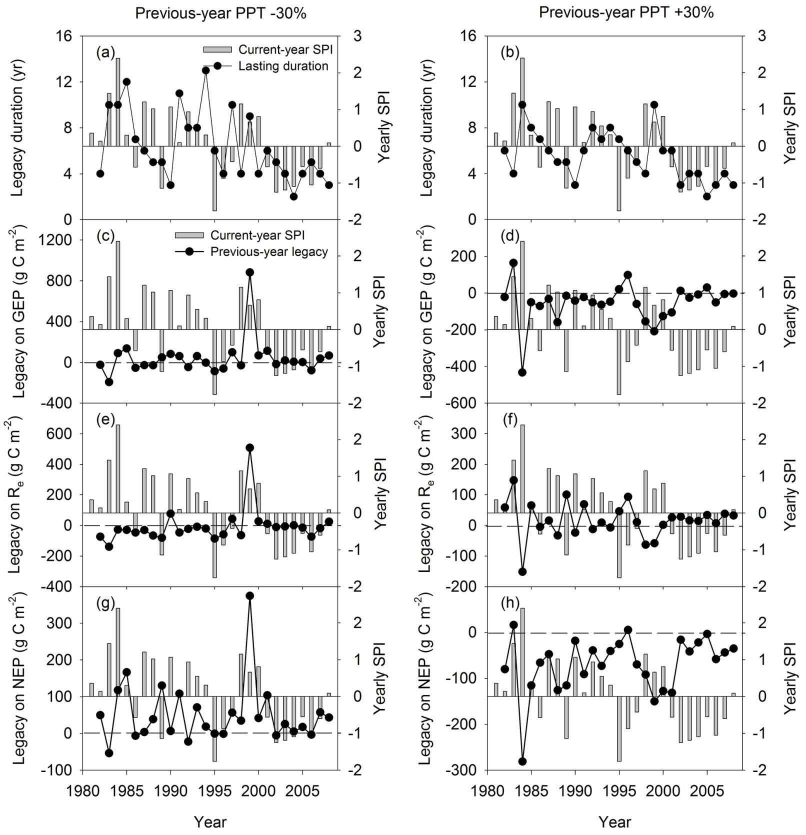

Figure 6. Interannual precipitation legacy effects on the ecosystem carbon fluxes. **(a)** and **(b)** show the lasting duration of dry (left panels) and wet (right panels) legacies, respectively. **(c)** through **(h)** show gross ecosystem production (GEP), ecosystem respiration (R_e) and net ecosystem production (NEP) responses. Bars in the background represent yearly standard precipitation index (SPI).

Title Page
Abstract | Introduction
Conclusions | References
Tables | Figures
◀| |▶
◀ ▶
Back | Close
Full Screen / Esc
Printer-friendly Version
Interactive Discussion

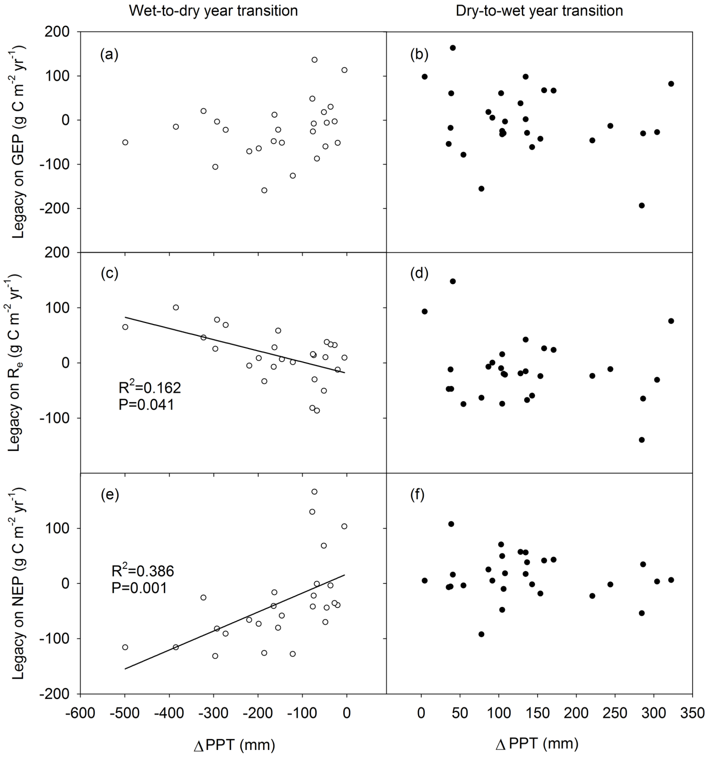

Figure 7. Spearman correlations of interannual precipitation legacy effects with the precipitation difference between years (Δ PPT). Interannual Δ PPT is calculated as current-year PPT minus previous-year PPT. Sample size is 26 for the wet-to-dry year transition (left panels) and 27 for the dry-to-wet year transition (right panels). GEP represents gross ecosystem production, R_e ecosystem respiration, and NEP net ecosystem production. R^2 is the coefficient of determination and P is probability.

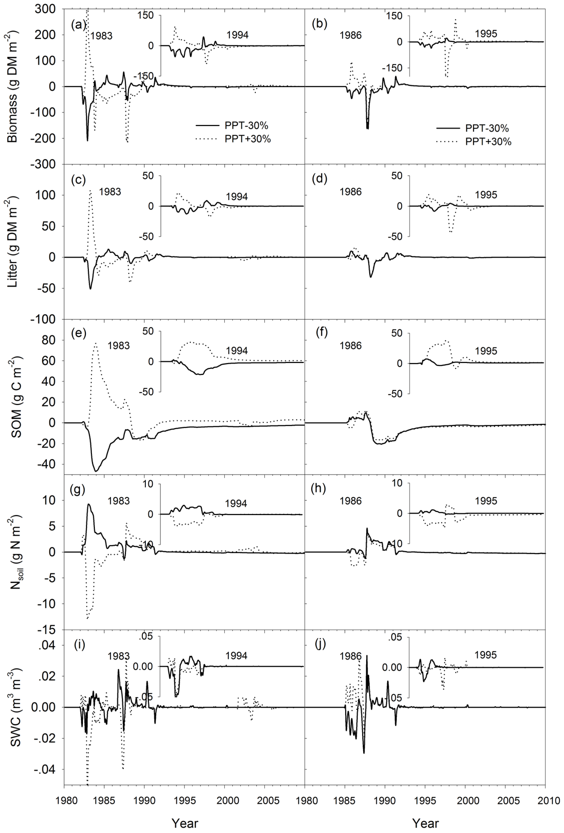

Figure 8. Interannual precipitation legacy effects on resource pool dynamics. Left panels show the legacy effects on pool dynamics in two representative wet years while right panels for two representative dry years. Solid lines represent a 30 % decrease while dashed lines represent a 30 % increase in the previous-year precipitation (PPT). SOM represents soil organic matter, N_{soil} soil mineral nitrogen, and SWC soil water content.